

# Heat transfer and thermal management of lithium-ion battery pack system with forced air convection

İ. Hoş<sup>1</sup>, G. Türkakar<sup>1\*</sup>

<sup>1</sup>Department of Mechanical Engineering, Zonguldak Bülent Ecevit University, Zonguldak, Turkey

## ARTICLE INFO

### Article Type:

Special Issue Article<sup>c</sup>

### Article History:

Received: 23 April 2021

Revised: 11 June 2021

Accepted: 27 June 2021

Published: 30 June 2021

### Editor of the Article:

Ö. N. Cora

### Keywords:

Battery cooling

Lithium-ion battery

Thermal battery management

Air forced convection

## ABSTRACT

Studies on battery cooling systems gain momentum every new year due to their limited operating temperature range. As lithium-ion batteries are one of the critical components of electric vehicles, researchers have recently focused on them. A two-dimensional analysis of a battery pack has been carried out in the current study. A hydrodynamic and thermal study was conducted for an air-cooled 6x6 battery pack (36 Lithium-ion 26650, LiFePO<sub>4</sub> batteries in total) system. The system was analyzed using the ANSYS / FLUENT software for aligned and staggered battery arrangements in steady-state conditions. The system's temperature distribution and pressure drop were scrutinized for constant volumetric flow rates of  $6.825 \times 10^{-3} \text{m}^3 \text{s}^{-1}$ ,  $10.238 \times 10^{-3} \text{m}^3 \text{s}^{-1}$ , and  $13.650 \times 10^{-3} \text{m}^3 \text{s}^{-1}$  for the aligned order. Same analyses were performed for the staggered order, with the help of keeping the mass flow rate constant. Numerical analyses were also performed for the discharge conditions of the batteries. Uniform and constant heat generation were assumed for the batteries during the discharge process. Heat generation was attributed as 1.43 W and 2.75 W per battery, corresponding to 2C and 3C discharge rates, respectively. The effect of battery arrangement and the air mean velocity on the temperature distribution and the total pressure drop in the system were inspected.

**Cite this article:** İ. Hoş, G. Türkakar, "Heat transfer and thermal management of lithium-ion battery pack system with forced air convection," *Turkish Journal of Electromechanics & Energy*, 6(1), pp.25-30, 2021.

## 1. INTRODUCTION

Electric vehicles (EVs) and hybrid electric vehicles (HEVs) have gained popularity, recently. Lithium-ion batteries are much more preferred than the other types of batteries due to their longer cycle and efficiency [1]. However, lithium-ion batteries have some drawbacks. In literature, it is known that the best operating temperature of lithium-ion batteries is 25-40 °C, and a maximum temperature difference of 5 °C in the battery pack is permitted [2]. Batteries generate heat while they are charged or discharged. If the generated heat could not be dissipated, it causes heat accumulation inside the battery, leading to an increment in the batteries' temperature.

As the fluid temperature increases in the streamwise direction, non-uniform temperature distribution might be observed in the battery pack. This non-uniformity may result in a breakdown in the battery system. Most importantly, some studies have indicated that the batteries' performance decreases with rising temperature [3, 4].

All these reasons explained above necessitate various types of cooling methods on the batteries. Many studies on cooling battery systems are available in the literature, such as liquid cooling, air cooling, cooling with phase change materials, and cooling with

heat exchangers. Each method has its advantages disadvantages. In this study, a battery pack cooling system with forced air cooling is investigated. There are many studies and comparisons about air cooling of the battery packs in the literature [5-8]. Sabbah et al. compared active (air cooling) and passive (phase change material) cooling methods [5]. They asserted that the air cooling without high fan power makes it impossible to dissipate heat, especially under high operating or ambient temperatures. On the other hand, using passive cooling techniques (e.g. phase changing materials) satisfies the operating temperature requirements. For this reason, forced convection cooling for battery packs needs special attention. It is crucial to achieve a uniform temperature distribution. Therefore, pack arrangement comes into prominence. Li et al. conducted experimental and numerical studies to determine the battery pack's maximum cell temperature and temperature variation. They have used the forced convection method. They indicated that the computational fluid dynamics (CFD) model and the experimental model showed consistency. However, they stated that optimization studies in the field should continue. Besides, they pointed out that different turbulence models and many parameters should be carefully investigated [6]. H. Park used a numerical model for forced air-cooled lithium-ion

<sup>c</sup>Initial version of this article was presented in the 5<sup>th</sup> International Anatolian Energy Symposium (5<sup>th</sup> AES), which was held in March 24-26, 2021, in Trabzon, TURKEY; and was subjected to a peer-review process before its publications.

\*Corresponding author e-mail: [turkakar@beun.edu.tr](mailto:turkakar@beun.edu.tr)

Science Literature™ © All rights reserved.

batteries in hybrid electric vehicles. Results indicated that the required cooling performance could be achieved using conical manifold and pressure relief ventilation [7]. Zhang et al. examined the air velocity effect on the battery pack system's temperature for different battery arrangements [8]. Mahamud and Park used reciprocating airflow to improve temperature homogeneity for a cylindrical Li-ion (LiMn204 / C) cell [9]. They aimed to reduce the maximum battery temperature; and used a 2D computational fluid dynamics CFD model. Also, they conducted experiments. They noted that a 3D CFD model would be much better to estimate the battery life and temperature.

He et al. performed experiments and numerical simulations to establish optimal cooling effectiveness regarding the maximum temperature rise, temperature non-uniformity between the cells, and reducing the parasitic power consumption [10]. They mounted two identical fans at both ends of the setup, creating reciprocating airflow in the battery module. Their optimization strategy was based on exploiting the reciprocating cooling flows. Results revealed that a combination of hysteresis control and reciprocating cooling flow could reduce the parasitic power by 84%. The temperature uniformity is enhanced, but a slight increment is observed in the cells. Lu et al. numerically analyzed the three-dimensional geometry of a staggered battery pack to investigate the effects of cooling channel size and air supply strategy on the 18650 li-ion battery pack's thermal behavior [11]. They sought the impact of the location of the inlet and the outlet ports on the thermal performance. They concluded that the best cooling performance was obtained if the airflow inlet and outlet are positioned at the top of the battery pack. They noted that packing more cells in the flow direction works very well in terms of the battery power density and cooling requirement. Although many studies related to forced air battery pack cooling in the literature, just a few of them have focused on the pack's temperature non-uniformity.

In this study, the air was used as the fluid. Battery pack temperature distribution and pressure drop were examined for different volumetric flow rates. Besides, the battery arrangement effect on the maximum temperature and the temperature uniformity was studied. There were 6x6 batteries located either aligned or staggered (36 batteries in total). Pressure drop and the pumping power were among the examined parameters investigated. Two different heat generation values were investigated. These were 1.43 W and 2.75 W corresponding to approximately 2C and 3C discharge rates of Lithium-ion 26650 LiFePO<sub>4</sub> batteries [12, 13]. It should be noted that the heat generation depends on the temperature and the state of charge of the battery, but some studies employ mean heat generation value during discharge [12, 13]. It is assumed that there is an uniform heat generation inside the batteries.

## 2. PROBLEM DEFINITION AND METHOD

Transient analysis of the cell pack was performed, yet the simulation was continued until the steady-state conditions were reached. A two-dimensional model was established. Air was used as a working fluid, and it flows along the x-direction as in Figure 1. The initial temperature of the batteries and the fluid inlet temperature were assumed as ambient temperature ( $T_{initial} = 296 K$ ). Symmetry boundary condition was

applied for the battery pack during the analysis to reduce the computational effort. Velocity inlet and pressure outlet boundary conditions were applied at the channel inlet and the outlet.

The geometry model is illustrated in Figure 1 (a) and (b) is demonstrated in detail for the aligned battery arrangement and the staggered battery arrangement, respectively.

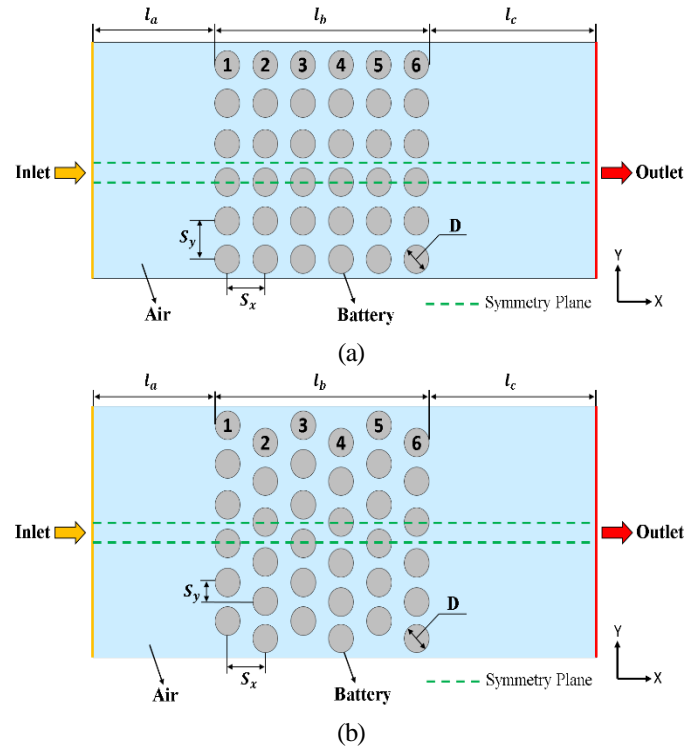


Fig. 1. Modelled 2-D Geometry, (a) Aligned arrangement, (b) Staggered arrangement.

The diameter of each battery cell is  $D = 26 mm$ . The distance between batteries in the x-direction is  $S_x = 35.2 mm$  and  $S_y = 35 mm$  in the y-direction for the aligned battery arrangement. For the staggered battery arrangement,  $S_x = 35.2 mm$  and  $S_y = 17.5 mm$ .

Moreover, the distance between the inlet and the first battery cell is  $l_a = 137 mm$ , and the distance between the outlet and the last battery cell is  $l_c = 237 mm$ , as projected in Figure 1. The total length of 6 batteries is  $l_b = 202 mm$ .

The meshed model was simulated in ANSYS Fluent 2019 R2 & 2021 R1 student versions. The equation of momentum and turbulent kinetic energy were discretized using the second-order upwind scheme. The Semi-Implicit Method for Pressure-Linked Equation (SIMPLE) algorithm was used for the pressure and velocity coupling. As a turbulent flow model, the  $k - \epsilon$  turbulence model (enhanced wall improvement) [6, 9] was used. Yang et al. employed the  $k - \epsilon$  turbulence model and validated the CFD simulations with experiments for similar volumetric flow rate values and the battery arrangement [8]. The mesh quality and size are important because it significantly improves the accuracy of the results. It is important to note that the boundary layer effect over the cylinder and the separation point is considered. The boundary layer thickness is adjusted based on the  $y^+$  value. Its

value was kept around 1.0 as it is done for enhancement wall treatment [6]. The inflation option with the value of 1.2 was used to compose the mesh structure within the boundary layer. The meshed geometry is given in Figure 2.

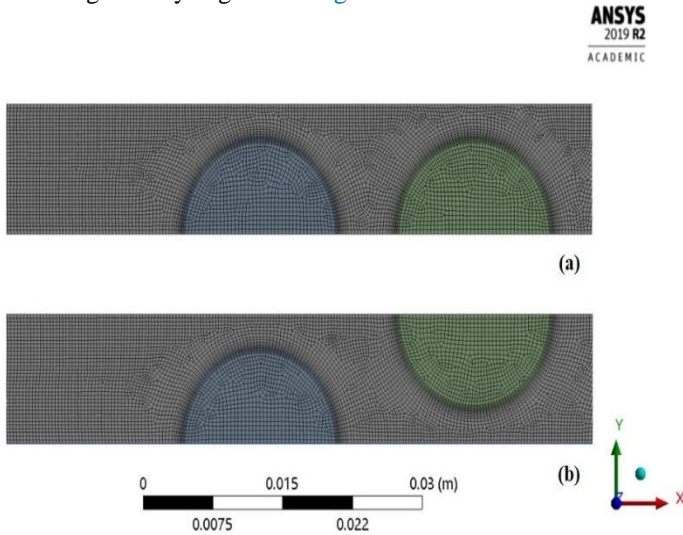


Fig. 2. Mesh model of design geometry (a) Aligned battery arrangement (b) Staggered battery arrangement.

Skewness, orthogonal quality, aspect ratio, and mesh element size for both modelled geometries are summarized in Table 1.

Table 1. Meshing and quality parameters.

Parameters	Aligned	Staggered
Skewness	0.60	0.69
Orthogonal Quality	0.65	0.62
Aspect Ratio	3.42	3.43
Element Size	40,093	39,803

The mesh independence is an essential parameter in CFD analysis and was verified in this study. If the mesh number (for the aligned arrangement in Figure 2, for 1.43 W heat generation) is increased by 60%, the system's maximum temperature changed approximately by 0.03%.

Mass, momentum, and energy equations for the two-dimensional airflow with negligible viscous dissipation and body force (in momentum eq) can be written as:

Continuity:

$$\frac{\partial \rho_a}{\partial t} + \nabla \cdot (\rho_a \vec{v}) = 0 \quad (1)$$

Momentum:

$$\frac{\partial}{\partial t} (\rho_a \vec{v}) + \rho_a (\vec{v} \cdot \nabla) \vec{v} = -\nabla P + \mu \nabla^2 \vec{v} \quad (2)$$

Energy:

$$\frac{\partial}{\partial t} (\rho_a C_{p,a} T_a) + \rho_a C_{p,a} (\vec{v} \cdot \nabla T_a) = \nabla \cdot (k_a \nabla T_a) \quad (3)$$

For the battery domain, the classical energy equation was employed with uniform and constant heat generation. In Table 2, the thermophysical properties of the fluid and the battery are summarized.

Table 2. Thermophysical properties of air (at T = 296 K) and battery.

Properties	Density kg m <sup>-3</sup>	Specific Heat Cap. J kg <sup>-1</sup> K <sup>-1</sup>	Thermal Conductivity W m <sup>-1</sup> K <sup>-1</sup>	Dynamic Viscosity kg m <sup>-1</sup> s <sup>-1</sup>
Battery [12]	2047	1075	3.91 [14]	-
Air	1.180064	1006.92	0.02598	1.826 · 10 <sup>-5</sup>

### 3. RESULTS AND DISCUSSION

#### 3.1. Temperature Distribution

The temperature values when the system reaches the steady-state regime at total (battery pack) volumetric flow rates of 6.825 × 10<sup>-3</sup> m<sup>3</sup>s<sup>-1</sup>, 10.238 × 10<sup>-3</sup> m<sup>3</sup>s<sup>-1</sup> and 13.650 × 10<sup>-3</sup> m<sup>3</sup>s<sup>-1</sup> for the aligned and staggered battery arrangement system are summarized in Tables 3, and 4 respectively.

When Tables 3 and 4 are examined, the temperature non-uniformity remained below the critical temperature value of 5°C for all 1.43 W heat generation cases. In the case of 2.75 W heat generation, it is seen that this critical value is exceeded at the lowest flow rate value for both battery arrangements. The non-uniform temperature distribution is observed for the volumetric flow rate value of 6.825 × 10<sup>-3</sup> m<sup>3</sup>s<sup>-1</sup> in the battery pack system for both arrangements.

When the temperature distribution is examined, it is seen for both battery arrangements that a more homogeneous temperature distribution was obtained for higher airflow rates.

Table 3. Battery temperatures at specified velocities for the aligned battery arrangement.

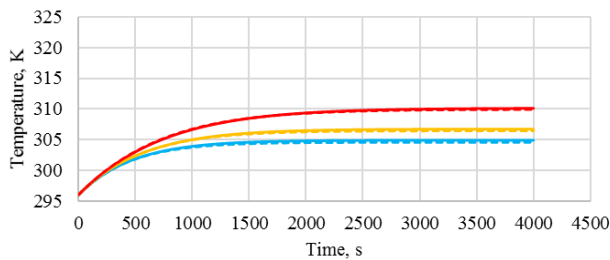
Aligned		Cell Temperatures, K (1.43 W)					
Vol. Flow Rate m <sup>3</sup> s <sup>-1</sup>	Velocity m s <sup>-1</sup>	Cell-1	Cell -2	Cell -3	Cell -4	Cell -5	Cell -6
6.825 × 10 <sup>-3</sup>	0.5	306.7	306.9	307.7	308.6	309.6	310.1
10.238 × 10 <sup>-3</sup>	0.75	304.6	304.8	305.2	305.8	306.5	306.7
13.650 × 10 <sup>-3</sup>	1	303.3	303.5	303.8	304.2	304.7	304.9
		Cell Temperature, K (2.75 W)					
6.825 × 10 <sup>-3</sup>	0.5	316.6	317.1	318.5	320.3	322.2	323.1
10.238 × 10 <sup>-3</sup>	0.75	312.5	312.9	313.7	314.9	316.1	316.6
13.650 × 10 <sup>-3</sup>	1	310.1	310.4	311.0	311.9	312.8	313.1

**Table 4.** Battery temperatures at specified velocities for the staggered battery arrangement.

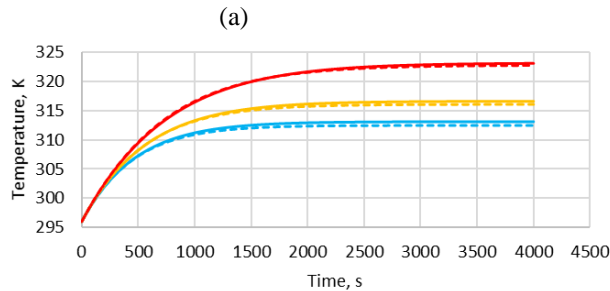
Staggered		Cell Temperatures, K (1.43 W)					
Vol. Flow Rate $m^3 s^{-1}$	Velocity $m s^{-1}$	Cell-1	Cell -2	Cell -3	Cell -4	Cell -5	Cell -6
$6.825 \times 10^{-3}$	0.46	306,3	305.0	306.5	307.6	308.8	309.9
$10.238 \times 10^{-3}$	0.69	304.2	303.1	304.2	304.9	305.7	306.4
$13.650 \times 10^{-3}$	0.92	303.1	302.1	302.9	303.4	304.0	304.6
		Cell Temperature, K (2.75 W)					
$6.825 \times 10^{-3}$	0.46	315.7	313.2	316.2	318.3	320.5	322.7
$10.238 \times 10^{-3}$	0.69	311.9	309.7	311.7	313.1	314.6	316.1
$13.650 \times 10^{-3}$	0.92	309.6	307.7	309.2	310.2	311.3	312.5

When Tables 3 and 4 are examined, slightly better heat removal was obtained for staggered battery arrangement. The heat transfer rate was slightly higher since the turbulence effect was promoted in this battery arrangement; hence, the staggered order's battery temperature values are lower. However, when the temperature distribution was studied, a more uniform temperature distribution was obtained for the aligned battery arrangement. This can be improved by modifying the distance between them. The last battery row in the flow direction was the most critical one in terms of temperature. Hence, only the 6<sup>th</sup> battery's transient analyses are provided in Figure 3.

The time-dependent temperature changes in the 6<sup>th</sup> battery row (the last battery row near to the outlet) for 1.43 W and 2.75 W heat generation are given for both battery arrangements in Figure 3 (a) and (b), respectively.



(a) 0.013650  $m^3/s$  (Aligned)      0.010238  $m^3/s$  (Aligned)  
 0.006825  $m^3/s$  (Aligned)      0.013650  $m^3/s$  (Staggered)  
 0.010238  $m^3/s$  (Staggered)      0.006825  $m^3/s$  (Staggered)



(b) 0.013650  $m^3/s$  (Aligned)      0.010238  $m^3/s$  (Aligned)  
 0.006825  $m^3/s$  (Aligned)      0.013650  $m^3/s$  (Staggered)  
 0.010238  $m^3/s$  (Staggered)      0.006825  $m^3/s$  (Staggered)

**Fig. 3.** Time-dependent battery temperature for the 6<sup>th</sup> battery (a) 1.43 W heat generation (b) 2.75 W heat generation.

The maximum allowable temperature difference between batteries also applies to the temperature non-uniformity in the battery itself. Accordingly, the temperature non-uniformity for a battery is also vital for the system. Thus, the temperature distribution inside the batteries ought to be investigated. Thanks to the red colour lines shown in Figure 4, temperature variation inside the batteries can be observed.

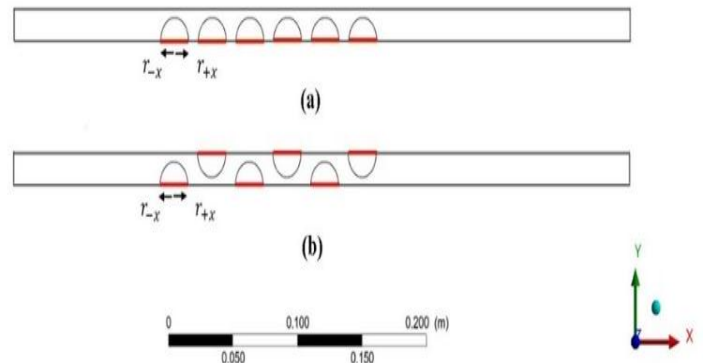


**Fig. 4.** The lines on which the temperature variation is examined, (a) Aligned battery arrangement, (b) Staggered battery arrangement.

The simulation was carried out at a flow rate of  $13.650 \times 10^{-3} m^3 s^{-1}$  and for 2.75 W heat generation. The temperature distribution inside the batteries for the steady-state regime is represented in Figure 5.

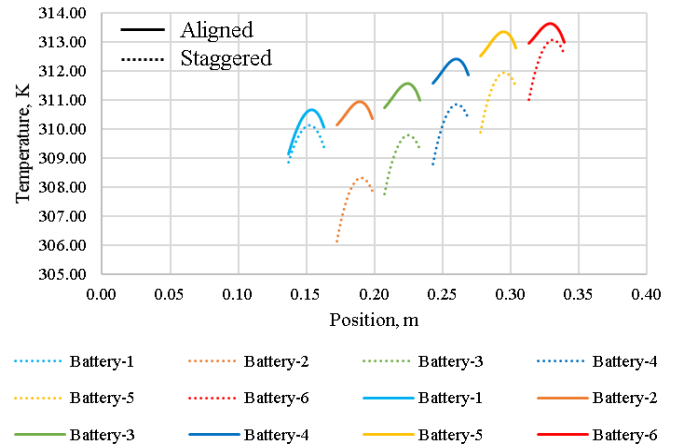


**Fig. 5.** Temperature change along the battery's diameter (For  $\dot{V} = 13.650 \cdot 10^{-3} m^3 s^{-1}$  and 2.75 W heat generation).

As it can be seen in Figure 5, while the temperature distribution is more uniform for aligned order, significant temperature variation in the batteries was observed for the staggered order. As the batteries meet the air in the upstream direction first, the temperature of that side of the batteries is lower in all cases.

Although the temperature values were quite close to each other for staggered and aligned orders for the first battery, battery arrangement comes to the foreground after the first battery. The turbulence effect gets dominated for the staggered order after the first battery row. Consequently, if a comparison is made for the same row, the average temperature of a battery is lower for the staggered order. Temperature contours of aligned battery order are provided in Figure 6.

Temperature variation in the air and the battery domain can be observed in Figure 6. Expectedly, the maximum temperature was observed in the last battery row, so it is better to keep the number of batteries high in the transverse direction. Otherwise, there is going to be significant temperature variation in the flow direction.

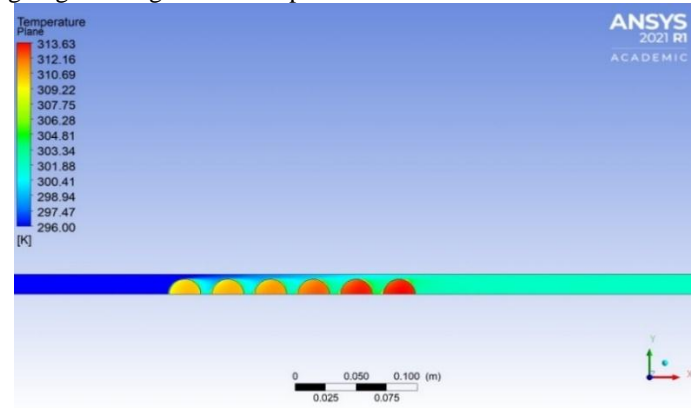


Fig. 6. Temperature contours of aligned, 2.75 W of heat generation,  $13.650 \times 10^{-3} \text{ m}^3 \text{ s}^{-1}$ , 4000<sup>th</sup> s (steady-state condition).

### 3.2. Pressure Drop and Cooling Index

The pressure drop through the battery pack is crucial for the design. Besides, pressure drop and pumping power are desired to be low in these systems. A cooling index parameter is defined as the ratio of the total heat rejection to the power consumed by the fan while the steady-state condition prevails [8]. Pressure drop, pumping power, and cooling index parameters are presented for different velocities in Table 5.

It can be concluded from Table 5 that the cooling index is better for the aligned order when compared to the staggering order at the same flow rate. Nevertheless, the average temperature observed in the aligned order is higher. Lower pressure drop and pumping power were the reasons behind the aligned order's better cooling index. As long as the operating temperature is in the safe range, the aligned order battery arrangement can be preferable due to its low fan energy consumption.

The velocity streamlines for the aligned battery order observes illustrated in Figure 7. As expected, the maximum velocity is obtained in the narrowest region of the battery pack, and the maximum speed of  $4.3 \text{ m s}^{-1}$  was noted. Vortex formation was formed in the downstream region.

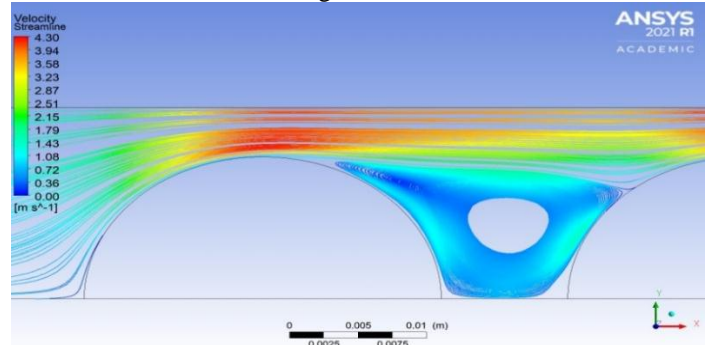


Fig. 7. Velocity streamlines of aligned, 2.75 W of heat generation,  $13.650 \times 10^{-3} \text{ m}^3 \text{ s}^{-1}$ , 4000<sup>th</sup> s (steady-state condition).

Table 5. Pressure drop, fan power, and cooling index values for both battery arrangements.

Vol. Flow Rate, $\text{m}^3 \text{ s}^{-1}$	Aligned				Staggered			
	Pressure Drop, Pa	Pumping Power, W	Cooling Index		Pressure Drop, Pa	Pumping Power, W	Cooling Index	
			1.43 W	2.75 W			1.43 W	2.75 W
$6.825 \times 10^{-3}$	5.7	0.0389	1323.4	2545	7.4	0.0505	1019.4	1960.4
$10.238 \times 10^{-3}$	11.5	0.1177	437.4	841.1	15.3	0.1566	328.7	632.2
$13.650 \times 10^{-3}$	18.5	0.2525	203.9	392.1	24.8	0.3385	152.1	292.5

## 4. CONCLUSION

The followings are the main conclusions from the current study conducted:

- The temperature difference between the batteries might be kept at a minimum level at high volumetric flow rates. By doing so, the temperature difference between the batteries is ensured to be under critical levels.
- The 6<sup>th</sup>-row battery owns the highest average temperature. When compared at the same flow rates, the average temperature is lower for the staggered order.
- Although the staggered order placement resulted in lower temperature values at the same battery row than the aligned order placement, temperature uniformity inside the batteries deteriorated.

- The cooling index is better for the aligned order than the staggered order at a constant flow rate. However, the average temperature observed in the aligned order was higher.
- As long as the operating temperature is in the safe range, aligned order battery arrangement can be preferred thanks to its low fan energy consumption.
- It is better to compromise from the cooling index and use at least an average flowrate ( $10.238 \times 10^{-3} \text{ m}^3 \text{ s}^{-1}$ ) for a 2.75 heat generation case as it much safer in terms of the cell temperature.
- The maximum temperature deviation between the cells during 2.75 W heat generation was noted as 4 °C for the aligned order. On the other hand, it was obtained as 7 °C for the staggered order.

## References

- [1] Y. Deng *et al.*, "Effects of different coolants and cooling strategies on the cooling performance of the power lithium-ion battery system: A review," *Appl. Therm. Eng.*, 142 (June), pp. 10–29, 2018.
- [2] A.A. Pesaran, "Battery thermal models for hybrid vehicle simulations," *J. Power Sources*, vol.110, pp. 378-382, 2002.
- [3] N. Sato, "Thermal behavior analysis of lithium-ion batteries for electric and hybrid vehicles," *J. Power Sources*, 99(1–2), pp. 70–77, 2001.
- [4] P. Ramadass, B. Haran, R. White, B. N. Popov, "Capacity fade of sony 18650 cells cycled at elevated temperatures Part I. Cycling performance," *J. Power Sources*, vol. 112, pp. 606–613, 2002.
- [5] R. Sabbah, R. Kizilel, J. R. Selman, and S. Al-Hallaj, "Active (air-cooled) vs. passive (phase change material) thermal management of high power lithium-ion packs: Limitation of temperature rise and uniformity of temperature distribution," *J. Power Sources*, 182(2), pp. 630–638, 2008.
- [6] X. Li, F. He, L. Ma, "Thermal management of cylindrical batteries investigated using wind tunnel testing and computational fluid dynamics simulation," *J. Power Sources*, vol.238, pp. 395-402, 2013.
- [7] H. Park, "A design of airflow configuration for cooling lithium-ion battery in hybrid electric vehicles," *J. Power Sources*, vol. 239, pp. 30–36, 2013.
- [8] N. Yang, X. Zhang, G. Li, and D. Hua, "Assessment of the forced air-cooling performance for cylindrical lithium-ion battery packs: A comparative analysis between aligned and staggered cell arrangements," *Appl. Therm. Eng.*, vol. 80, pp. 55–65, 2015.
- [9] R. Mahamud and C. Park, "Reciprocating airflow for Li-ion battery thermal management to improve temperature uniformity," *J. Power Sources*, 196(13), pp. 5685–5696, 2011.
- [10] F. He, H. Wang, L. Ma, "Experimental demonstration of active thermal control of a battery module consisting of multiple Li-ion cells," *Int. J. Heat. Mass Tran* vol. 91, pp. 631-639, 2015.
- [11] Z. Lu *et al.*, "Parametric study of forced air cooling strategy for lithium-ion battery pack with staggered arrangement," *Appl. Therm. Eng.*, 136 (February), pp. 28–40, 2018.
- [12] A. Lazrak, J. F. Fourmigué, and J. F. Robin, "An innovative practical battery thermal management system based on phase change materials: Numerical and experimental investigations," *Appl. Therm. Eng.*, vol. 128, pp. 20–32, 2018.
- [13] C. V. Hémerly, F. Pra, J. F. Robin, and P. Marty, "Experimental performances of a battery thermal management system using a phase change material," *J. Power Sources*, vol. 270, pp. 349–358, 2014.
- [14] Zhao, J., Rao, Z., Huo, Y., Liu, X. & Li, Y., "Thermal Management of Cylindrical Power Battery Module for Extending The Life of New Energy Electric Vehicles," *Applied Thermal Engineering*, vol. 85, pp. 33-43, 2015.

## Biographies



**İsmail Hoş** received a B.Sc. degree from Mechanical Eng. Dept., Zonguldak Bülent Ecevit University, in 2019, Zonguldak Turkey. He is continuing to his M.Sc. degree studies at Zonguldak Bülent Ecevit University. He worked for about one year ITFS Mühendislik A.Ş., which has been doing R&D studies on heat pipes. Afterwards, he worked as a Mechanical Design Engineer in an R&D project at TEKGEN Health Services Limited Company for six months. His main research interest is the heat transfer.

**E-mail:** [ismaill.hoss@gmail.com](mailto:ismaill.hoss@gmail.com)



**Göker Türkakar** obtained his B.Sc. degree from Mechanical Eng. Dept. of Osmangazi University, in 2006, Eskisehir Turkey. He obtained his M.Sc. in 2010 from Mechanical Eng., Middle East Technical University (METU), Ankara, Turkey. He was awarded with Ph.D. degree from Mech. Eng., METU in 2016. He joined to Thermal Analysis, Microfluidics and Fuel Cell Lab at Rochester Institute of Technology in March 2015 (9 months) as a visiting scholar. He focused on designing a microscale refrigeration cycle for electronics cooling in his Ph.D. study. He works as a faculty member in the Mechanical Department of Zonguldak Bülent Ecevit University since 2017.

**E-mail:** [turkakar@beun.edu.tr](mailto:turkakar@beun.edu.tr)